J Therm Spray Tech (2022) 31:685–698
https://doi.org/10.1007/s11666-022-01330-2

PERSPECTIVE

A Perspective on Thermally Sprayed Thermal Barrier Coatings: Current Status and Trends

Robert Vaßen[1,2] · Emine Bakan[1] · Daniel Emil Mack[1] · Olivier Guillon[1,3]

Submitted: 29 October 2021 / in revised form: 7 December 2021 / Accepted: 8 December 2021 / Published online: 22 February 2022

Abstract For more than 6 decades, thermal barrier coatings have been used to protect structural parts in both stationary and aviation gas turbines. These coatings allow the use of significant higher operation temperatures and hence increased efficiencies. In the 1970s, yttria-stabilized zirconia (YSZ) was identified as outstanding material for this application. As major deposition technologies both electron beam physical vapor deposition (EB-PVD) and atmospheric plasma spraying (APS) have been established. Although the topic is already rather old, there are still frequent activities ongoing to further improve the technology, both with respect to materials and microstructural issues also regarding the use of advanced coating technologies, especially in the field of thermal spray. The paper tries to summarize major developments in both fields, the materials and the processing focusing on thermal spray methods. The impact of both materials and processing are summarized by the results of burner rig tests for various systems. Furthermore, a short outlook on possible future directions of developments will be given.

Keywords thermal spray · materials · burner rig test · lifetime · thermal barrier coatings · yttria-stabilized zirconia

Introduction

The authors are aware that already a number of excellent review articles on thermal barrier coatings exist (Ref 1-6). However, the authors believe that a comparative evaluation of the present status and the discussion of innovative directions of development was only partially presented up to now.

A major driving force for the development of advanced thermal barrier coatings was the wish to further improve the efficiency and by that reduce fuel consumption and CO_2 emissions. Over several decades, the improvement of the structural materials from wrought, conventionally cast, directionally solidified to single-crystal alloys could generate a considerable increase in operation temperature (Ref 7). A further significant increase could be achieved by the use of thermal barrier coatings in combination with advanced cooling technologies. Alternatively, the use of TBCs can reduce the substrate temperature and hence increase the lifetime of the components (Ref 9). In practice, a combination of both strategies is applied. The full use of the temperature capability would imply a prime reliant TBC system in combination with a well-developed lifetime prediction methodology. This last topic is still an issue although it is the content of intense research for many years (Ref 10-16). However, it will not be addressed in the present paper.

This article is an invited paper selected to provide expert perspectives on a target subject relevant to thermal spray. The views expressed in the paper are those of the author(s). It is also part of a special issue focus in the Journal of Thermal Spray Technology celebrating the 30th anniversary of the journal. The papers and topics were curated by the Editor-in-Chief Armelle Vardelle, University of Limoges/ENSIL.

✉ Robert Vaßen
r.vassen@fz-juelich.de

[1] Forschungszentrum Jülich GmbH, Institute of Energy and Climate Research IEK-1, 52425 Jülich, Germany

[2] Ruhr-Universität Bochum, Institute for Materials, Bochum, Germany

[3] Jülich Aachen Research Alliance, JARA Energy, Jülich, Germany

The development of thermal barrier coatings started in the 1950s using enamel coatings in military engines (Ref 17); then, in the 1960s the first thermal spray coatings were used. A major step forward was the identification of partially yttria-stabilized zirconia (YSZ with 4-5 Mol.-% Y_2O_3) as a unique material for thermal barrier coating application (Ref 18, 19) in the 1980s of the last century. YSZ is now since 4 decades the standard material for TBC applications (Ref 20). YSZ has a number of unique properties, which fit excellently to the needs of a thermal barrier coating system. Several of these properties such as low thermal conductivity, high thermal expansion coefficient, good processability, good compatibility with the oxide scale (alumina) growing on bond coats (see below) or low sintering rates have been intensively discussed in several review articles (Ref 6, 21, 22) and will not be repeated here. Some properties of new TBC materials will be discussed in the advanced TBC materials chapter.

However, some properties of YSZ are mentioned here as they are important also for future developments. One important property is the high fracture toughness of 4-5YSZ TBCs coatings. The values are lower than those observed at low temperatures in fine-grained sintered so-called tetragonal zirconia poly-crystal (TZP) material (Ref 23), however, considerably higher than the values of fully stabilized 8YSZ used in solid oxide fuel cells. Unfortunately, the high toughness values of TZP are not found at elevated temperatures in TZP as then the driving force for the transformation toughening is missing. Here the metastable t´-phase, which is developed during both thermal spray and PVD processing, plays a key role. It has been shown that this microstructure leads to a ferroelastic toughening mechanism, which provides sufficient toughness even at higher temperatures (Ref 24). This toughness is unique compared to most alternative materials which were investigated during the last decades. However, during long-term use at elevated temperatures, typically 1200 °C is given as limit, massive diffusion is observed and the t´-phase decomposes into tetragonal and cubic phases (Ref 25). The tetragonal phase then shows detrimental phase transformation to the monoclinic phase during cooling. Interestingly, a recent paper shows that the influence of the monoclinic phase in the spray powder is only of minor importance (Ref 26) for phase stability. New materials were investigated to overcome the limitation in the thermal stability of YSZ also with respect to sintering issues. The identified materials are often advantageous with respect to, e.g., lower thermal conductivity, improved corrosion resistance or better high-temperature stability; however, the lack of toughness often implies that new ceramics have to be applied in a double-layer structure. A YSZ layer on top of the bond coat is used here at the interface, where most often failure occurs and high toughness is needed (Ref 27). Chinese colleagues in most cases call this a double-ceramic-layer (DCL) structure (Ref 28-30). More details on the application of new TBC ceramics including pyrochlores or high-entropy oxides will be given in this paper.

For the manufacture of thermal barrier coatings, mainly two methods are commercially used: thermal spray methods and electron beam–physical vapor deposition (EB-PVD). The EB-PVD process leads to columnar structured topcoats with a high strain tolerance (Ref 30, 31). These typically rather thin coatings of about 200µm are used on the blades of the first row of the high-pressure turbine of aero engines.

For many other locations as combustion chambers and transition ducts in aero engines and nearly all parts in stationary gas turbines, thermally sprayed coatings are used with thickness values typically considerably larger than 200 µm (Ref 32). This deposition process will be the focus of this paper. Often it is emphasized that the performance of EB-PVD coatings is much better than thermally sprayed ones (Ref 33). However, if one considers also the possible larger thickness and the lower conductivity, the advantage is certainly reduced (Ref 34). Furthermore, compared with burner rig results also the performance of several thermally sprayed systems is similar to EB-PVD systems as will be shown in the paper.

The most often used thermal spray technique is atmospheric plasma spraying (APS). Due to the high enthalpy of the plasma plume, the high-melting-point YSZ powder can be easily fully molten which is essential for a highly efficient deposition. The process allows the manufacture of porous and micro-cracked as well as segmented (or also called dense vertically cracked—DVC) coatings. Further flexibility in the coating microstructure can be obtained by using suspension plasma spraying (SPS, columnar or porous/segmented) and plasma spray–physical vapor deposition (PS-PVD, columnar). The different features will be discussed not only with respect to thermomechanical properties in the as-processed condition but also as they are compromised by sintering or by corrosion from molten silicate deposits (which are often called CMAS after their main components CaO-MgO-Al_2O_3-SiO_2 (Ref 35)).

Thermal barrier coating systems do not only consist of the isolative ceramic topcoat, but also use a metallic bond coat (Ref 36). The bond coat used in thermal spray typically is made of nickel- and cobalt-based alloys with a large amount of aluminum and chromium (NiCoCrAlY) to form a protective alumina scale (thermally grown oxide—TGO) during operation. The addition of so-called reactive elements (like Y) improves the scale adhesion and reduce oxidation rates (Ref 37). By forming a slow-growing protective scale, the bond coat protects the substrate from oxidation and also corrosion. In addition, the bond coat deposited by thermal spray techniques such as vacuum

plasma spraying (VPS), high-velocity oxy fuel (HVOF) or atmospheric plasma spraying (APS) has a rough surface with R_a values larger than 6 and often larger than 10 µm leading to a good interlocking and hence adhesion of the topcoat to the bond coat. Typically, longer lifetimes are observed for increased bond coat roughness (Ref 38). In this paper, additional approaches, like applying of so-called flash coats, surface structuring, e.g., by laser ablation or laser cladding, to improve the surface profile of the bond coat will be discussed to some extent.

For the evaluation of the performance of TBC systems, different methods such as furnace cycle or also burner rig testing (Ref 39) are used. While the furnace tests mainly analyze failure due to bond coat oxidation (Ref 40), in burner rig testing additionally the effect of realistic gradients through the topcoat and fast cooling and heating rates can be considered. Even more realistic tests like thermal mechanical fatigue (TMF) or thermal gradient mechanical fatigue (TGMF) also consider mechanical loading of the TBC system and are hence very close to the thermomechanical loading in application (Ref 41). However, due to the complexity and the costs of the tests, only limited data are available. For the discussion of different TBC systems, in this paper results of burner rig tests are compared (Ref 42).

Advanced TBC Materials and their Application

In order to meet the continuously increasing hot gas temperature demand in the gas turbine engine industry, alternative ceramic materials for replacing the partially yttria-stabilized zirconia TBC topcoat have been investigated (Fig. 1). Among these materials are yttria-stabilized zirconia with additional dopants such as titania (Ref 43-45), tantala (Ref 46, 47), fully stabilized zirconia with yttria (12 wt. %YSZ (Ref 48)) or ceria (25 wt.% CeSZ (Ref 48)), zirconia stabilized with multiple components in addition to yttria such as Nd_2O_3, Gd_2O_3, Sm_2O_3 and Sc_2O_3 (Ref 49-51), pyrochlores and fluorites (Ref 52-65), perovskites (Ref 66-71), aluminates (Ref 72-74), phosphates (Ref 75, 76) and high-entropy oxides which will be further discussed below. Figure 1 compares the thermal conductivity and coefficient of thermal expansion (CTE) of these materials or coatings and partially yttria-stabilized zirconia (Ref 77-79). Thermal conductivity is desired to be as low as possible to ensure maximum thermal insulation while the expansion coefficient should be as close as possible to the substrate material to minimize stresses. In addition to these, there are many other essential requirements to meet such as high-temperature phase stability, high sintering onset temperature, high fracture toughness, low elastic modulus and chemical compatibility with TGO alumina and YSZ (if two materials will be combined). The list gets longer if the extrinsic degradation mechanisms like CMAS corrosion are considered. The new materials are typically proposed based on their high-temperature phase stability and low thermal conductivity (e.g., $Gd_2Zr_2O_7$ pyrochlore); however, it is often the case that they lack some other properties (e.g., fracture toughness). To exploit the best of each material and to answer the different needs of various operating conditions, therefore, workarounds are employed. For instance, if the thermal conductivity of the material is not low enough to ensure sufficient thermal insulation, the coating thickness might be increased at least if elastic modulus and CTE of the same material allow avoiding high stresses in the rather slowly heated coating system. If the material has a low fracture toughness, a second layer made of a material with higher resistance to crack propagation (e.g., YSZ) is used close to the locations where the failure most often occurs, namely at the bond coat topcoat interface (Ref 80-83). It should be also mentioned that some of the material properties can be also altered by microstructural modifications. For instance, thermal conductivity and elastic modulus can be lowered with increased porosity while sintering becomes less critical for a dense vertically cracked microstructure (Ref 84-88). Using these different strategies by combining the advances in materials and microstructure developments, more challenging operating conditions were established within the last decades leading to increased efficiency in gas turbine engines.

High-entropy oxides (HEO) which oftentimes refer to a high configurational entropy but not necessarily an entropy-stabilized oxide (ESO) in the literature are the newest high-temperature material category for TBC application. Entropy-stabilized oxides are named after the study of Rost et al. (Ref 89) in 2015 wherein it is said that the authors drew inspiration for this study from high-entropy alloy (HEA) activities. Rost et al. demonstrated the reversible low-temperature multiphase to high-temperature single-phase rocksalt structure transformation, which is a requirement for entropy-driven transitions, for a material system consisting of an equimolar mixture of MgO, CoO, NiO, CuO and ZnO. In the following years, many studies investigating oxides with five components stabilized into a single-crystal structure that can differ from the typical crystal structures of the constituent elements and which may or may not show the reversible phase transition were published. In these studies, HEO and ESO terms were interchangeably used by the researchers leading to some confusion. Definitions of these two fundamentally different concepts and formation criteria of single phases are discussed in detail in the recent reviews (Ref 90, 91). From the TBC application perspective, it is clear that high-temperature phase stability of the oxide is essential, and reversible multi-single-phase transitions, if any, under long-term

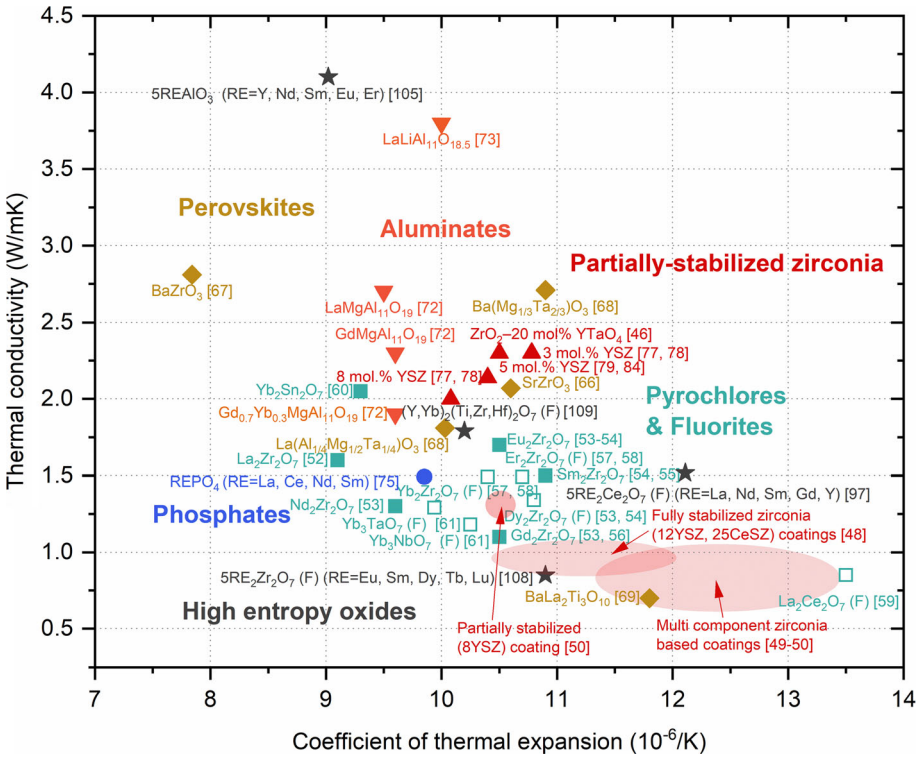

Fig. 1 Coefficient of thermal expansion (CTE) vs. thermal conductivity of different TBC topcoat materials. Thermal conductivities of dense materials or normalized thermal conductivities from the coatings with a known porosity are shown in the graph (for the plasma sprayed coatings marked by the arrows, no normalization was made). Given CTE values are in between RT-(1000-1300 °C) and thermal conductivity values are at 900–1000 °C (in ref [105] at RT)

thermal cycling conditions should require systematic investigations. Furthermore, research on powder synthesis and coating processing routes and the effect of these on the phase stability and other properties of such multi-component oxides is imperative to develop advanced coating systems for the future.

Since 2017, HEOs based on transition metal oxides, rare earth oxides or a mixture of these two with 5 or more cations stabilized into different crystal structures including fluorite (Ref 92-98), pyrochlore (Ref 99, 100), spinel (Ref 101, 102) and perovskite (Ref 103-105) have been reported in the literature. On multiple occasions, lower room temperature thermal conductivities of the synthesized HEO than that of the YSZ were demonstrated, i.e., Chen et al reported thermal conductivity of $(Ce_{0.2}Zr_{0.2}Hf_{0.2}Sn_{0.2}Ti_{0.2})O_2$ to be 1.28 Wm^{-1} K^{-1} (Ref 93), Zhao et al. measured thermal conductivity of $(La_{0.2}Ce_{0.2}Nd_{0.2}Sm_{0.2}Eu_{0.2})_2Zr_2O_7$ as low as 0.76 W m^{-1} K^{-1} (Ref 100), Wright et al. determined thermal conductivity of $Hf_{0.284}Zr_{0.284}Ce_{0.284}Y_{0.074}Ca_{0.074}O_{2-\delta}$ as 1.54 Wm^{-1} K^{-1} (Ref 96), and finally, Xu et al. reported thermal conductivity of $(La_{0.2}Sm_{0.2}Er_{0.2}Yb_{0.2}Y_{0.2})_2Ce_2O_7$ as 1.8 Wm^{-1} K^{-1} (Ref 98). According to the study of Lim et al., phonon scattering from mass and charge disorder is responsible for the reduced thermal conductivity in ESOs and the latter has a larger contribution (Ref 106). Zhao et al. reported slower grain growth in $(La_{0.2}Ce_{0.2}Nd_{0.2}Sm_{0.2}Eu_{0.2})_2Zr_2O_7$ in comparison with $La_2Zr_2O_7$ under the same annealing conditions (Ref 100). Based on that, the authors suggested a better sintering resistance in the HEO and attributed it to sluggish diffusion which is an often used term in the HEA literature yet hard to prove due to complex diffusion paths of multiple components (Ref 107). Similarly, Xu et al. experimentally observed a better sintering resistance of $5RE_2Ce_2O_7$ (RE=La, Gd, Er, Yb, Y) when compared to $La_2Ce_2O_7$ (Ref 97). Although these are promising results, some other characteristics of HEOs that are crucial for TBC application such as phase stability under thermal cycling conditions, CTE (only reported in a few studies (Ref 97, 105, 108, 109) which are shown in Fig. 1), mechanical properties (e.g., elastic modulus and toughness which were also measured rarely (Ref 96, 109)) remain to be explored in the future.

Different Plasma Sprayed TBC Topcoats

Thermal spray technologies offer a huge flexibility in microstructure, especially for ceramic coatings (Ref 110). The most often used one for TBC application is the lamellar, micro-cracked structure (Fig. 2a). The coating shown has a porosity level of about 15% (Ref 111). The micro-cracks allow by a slight sliding of the splats in the lamellar microstructure even at room temperature a considerable degree of viscosity (Ref 112) and hence the ability to relax stresses. Furthermore, the cracks reduce

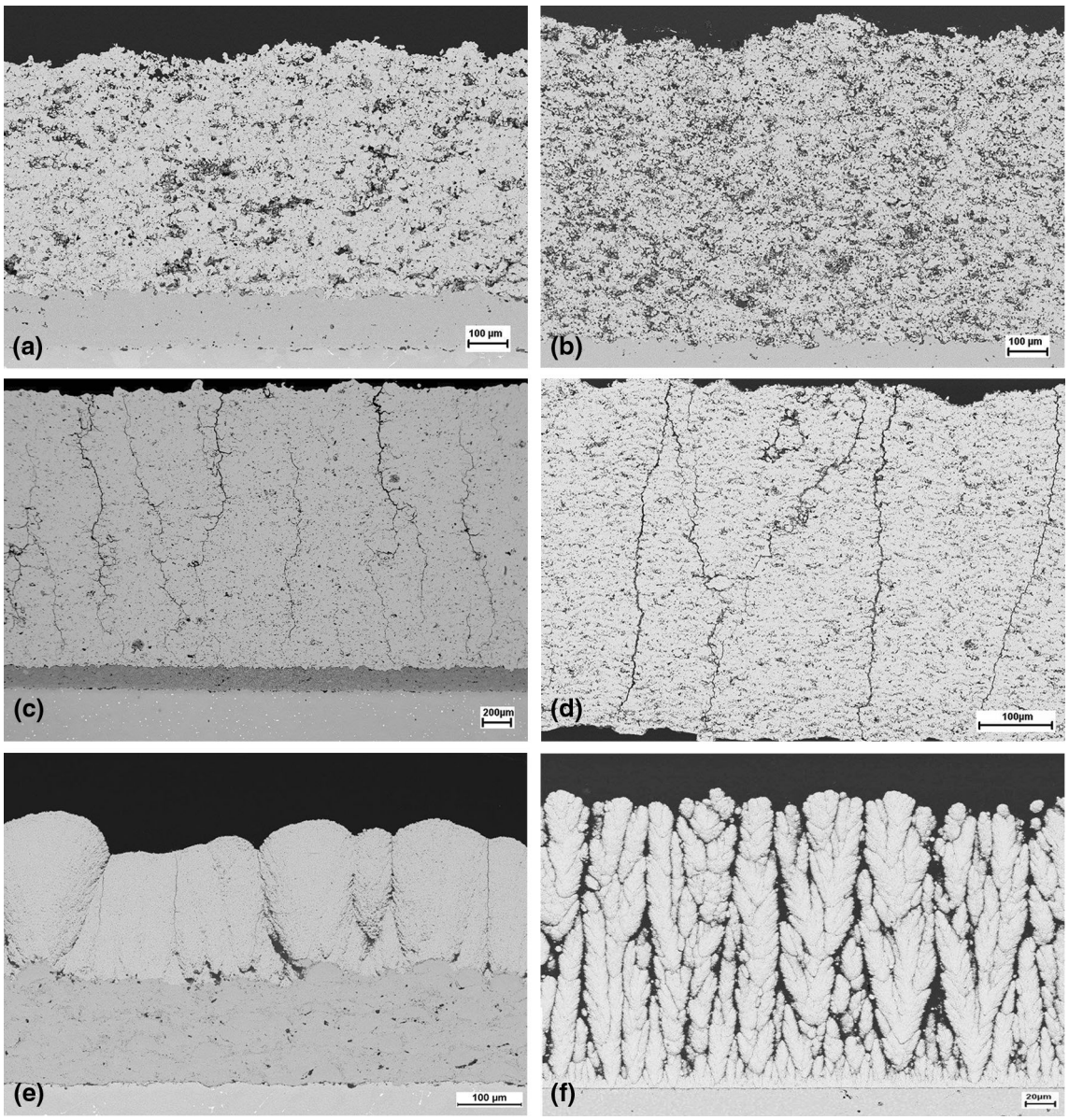

Fig. 2 Different thermally sprayed YSZ thermal barrier coatings: (a) conventional APS (medium porosity level), (b) highly porous APS, (c) thick segmented APS, (d) segmented SPS, (e) columnar SPS, (f) columnar PS-PVD

efficiently the thermal conductivity (Ref 113, 114). Typically such coatings in the thickness range of several hundred microns are used in the high-pressure turbine. Thicker coatings are of interest, especially in the combustion chamber or also as abradable seals (Ref 115, 116). However, in stationary engines also thicker coatings are nowadays applied on blades and vanes as shown in Table 1 and discussed later. For thick coatings approaching 1 mm or more, the stresses in the coatings (which are typically somewhat reduced compared to thin coatings!) lead to high energy release rates. This elastically stored energy in the coatings is typically proportional to the coating thickness and is often the driving force for spallation. One possibility to reduce the energy release rate is the reduction of the Young's modulus by the further increase of porosity levels up to 25% (Ref 117) or higher also by using additional polymers (Ref 118, 119). An example of a highly porous coating (23% porosity) is given in Fig. 2(b). The use of such highly porous coatings has also some drawbacks as the coating integrity is reduced leading, e.g., to lower erosion resistance, and also the deposition efficiency is reduced; hence, costs increase (Ref 120). Another approach is the use of segmented or also called dense vertically cracked (DVC) coatings. These coatings are produced

Table 1 Properties and temperature values for thermal barrier coatings applied in aero and stationary gas turbines, por—porous, seg—segmented, ATBC= advanced TBC materials typically applied by APS as double layer: new material (e.g., pyrochlores, fully stabilized YSZ) / YSZ by or also as single layer in EB-PVD. Further discussion is found in the materials section.

Component		Main material used	Main coating tech. used	Tmax surface [°C]	Tmax bond coat [°C]	Coating thickness [µm]	Porosity levels [%]
Aero engines	Blades and vanes	YSZ or ATBC	EB-PVD APS (2. vane)	<1300	950–1050	50–200	Low
	Combustion chamber	YSZ	APS	<1300	<950	200–250	15–20
Stationary gas turbines	Blades and vanes	YSZ or ATBC	APS	YSZ >1300, ATBC above 1500 (locally)	Approaching. 1000°C	300–500 old, 500–1000 new	15–20, 15–20 (new)
	Combustion chamber	YSZ	APS-por	<1500°C	<<1000°C	1000–2000	15–25
			APS-seg	<1350°C	<<1000°C	1000–1500	<5

under rather hot spraying conditions with high substrate temperatures which allow an excellent bonding of the splats. Hereby, quenching stress relaxation is not possible as in ordinary APS coatings and segmentation cracks are developed (Ref 121, 122). An example of a thick segmented coating is found in Fig. 2(c). Already older results for about 2-mm-thick coatings show that there is a benefit of these types of coatings compared to conventionally ones (Ref 123, 124). Similar as in columnar EB-PVD coatings, the tensile stress level at elevated temperatures is reduced, leading to reduced relaxation and hence reduced compressive stress after cooling (Ref 6). However, the segmented coatings show, due to their low porosity levels, higher thermal conductivities ($\sim$1.5 W/m/K) compared to porous ones (< 1W/m/K). Hence, thicker coatings are needed for the same cooling effect, and at a certain thickness, also this concept is at an end. In fact, only the surface of the segments are really stress-free, the inner part of the segments still see, although reduced, stresses and these can lead to failure at a certain coating thickness.

In Table 1, an overview of the different described types of thermal barrier coatings with relevant temperature ranges is given. The table is based on an older version published in 2000 (Ref 125) and was updated and extended to aero engines according to the information given by a number of industrial colleagues and by available information in the literature (e.g., Ref 2, 126-128).

Another coating technology which was intensively studied during the past decades is the suspension plasma spraying. This process was developed first in the 1990s in a number of institutions, a list is found in (Ref 129). Due to the use of suspensions as feedstock, this process allows the manufacture of new, often more fine-scale microstructures compared to the conventional APS. In the process, the suspension is atomized in the injection nozzle and then further fragmented by the plasma jet. The established droplet size, which is a key parameter to control the microstructure, is depending on various process parameters such as injection and plasma conditions, suspension solid loading and viscosity. Hence, the process is even more complex than the APS process and, on the other hand, allows a large variation in the microstructure. In contrast to APS, the Stokes number, which describes whether the particle/droplet can follow the gas flow, comes into play. For larger Stokes' numbers as for larger droplets or fast gas flows that is not the case and the droplets impinge directly on the substrate. So they form a dense or porous layer depending on the molten state of the deposited species. As the species are rather small, the tendency for crack formation is reduced; hence, also relaxation processes cannot reduce quenching stresses so effectively. As a result, one can produce segmented coatings even with a high porosity level ((Ref 130), Fig. 2d).

For about a decade the capability of the SPS process to produce columnar coatings has also attracted large interest (Ref 131). This structure (see Fig. 2e) is expected to give high (tensile) strain tolerance, and they should show improved thermal cycling performance. In fact, promising results have been shown, especially in furnace cyclic tests and thermal shock tests (Ref 132). The large number of industrial patent applications in the field (Ref 129) also clearly shows the interest of the industry. In (Ref 133), the good performance of SPS TBCs also compared to EB-PVD TBCs is demonstrated in furnace cycling tests. Furthermore, the technology is applied to complex shaped parts; clearly, the specific growth conditions need optimized spray processes, especially with respect to the movement of the spray gun. As an advantage, it should be mentioned here that the process conditions leading to columnar like structures have a non-line-of-sight capability. Although

columnar SPS TBCs appear to be very attractive coatings for thermally loaded parts, it was also stated that under harsh burner rig conditions with fast heating and cooling regimes and additional substantial TGO formation, the performance appears even worse than this of APS coatings. This was recently demonstrated in (Ref 134) and will be further discussed in the burner rig performance part. Under the specific burner rig conditions combing gradient testing and massive oxidation of the bond coat, the above-mentioned segmented, porous SPS TBC perform somewhat better; however, they still do not reach the performance of APS coatings for rather thin coatings.

As a last new deposition process, the plasma spray–physical vapor deposition (PS-PVD) will be described. This process, developed by Oerlikon Metco (Ref 135), uses specific feedstock material, which disintegrates during feeding, and the generated fine particles are then in the high-power plasma torch not only molten but also evaporated. Hence, a true gas phase deposition is the result, which can lead to the growth of columns, which are even single crystals under specific conditions (Ref 136). This deposition process also needs smooth bond coats, and the bonding mechanism is mainly a chemical one. Due to the unique microstructure (see Fig. 2f), these coatings show an excellent performance in harsh thermal cyclic conditions, which is shown in the later part of the paper. Due to the need of vacuum condition for the deposition process, it is certainly more expensive than APS or SPS; however, it is expected that the high powder feeding rates and an optimized coating procedure adopted to the specific components might gain a cost–benefit compared to EB-PVD. In addition, a major benefit of the process is its non-line-of-sight capability, which also allows the coating of complex shaped components. Most of the installed PS-PVD facilities are located in China, where the technology attracted a lot of interest in the last decade. It should also be mentioned here that slightly reduced power regimes lead to a more conventional plasma spraying process, however, with very high particle temperatures and velocities which offer the possibility to produce gas tight coatings (Ref 137). This process is nowadays used for the deposition of excellent crystalline and dense environmental barrier coatings (Ref 138).

Mitigation of CMAS-Induced Degradation

A critical aspect in the ongoing development of modern TBC systems is the protection of the integrity of the ceramic layers against the attack by deposits of sand or volcanic ash particles (CMAS), which become liquid at temperatures above approximately 1200 °C. The ceramic layers of the TBC systems can in general be affected by these deposits in two ways: First, the melt infiltrates the open microstructure of the ceramic and the porosity of the infiltrated ceramic layers is reduced. Second, the chemical interaction with the melt can lead to the formation of a reaction zone or an increased sintering rate of the ceramic layers. Such densification of the microstructure usually increases the thermal conductivity of the barrier layer. Most importantly, the solidification of the melt at lower temperatures, the formation of dense reaction zones and also the increased sintering rate lead to a stiffening of the structure, which directly increases the energy release rate, and thus the driving force for spallation of the stiffened layers (Ref 139, 140).

Considering this, efforts are being made to optimize both the composition and microstructure of TBCs for increased resistance to degradation by CMAS. When using or additionally applying topcoat materials that show rapid formation of a passivating reaction layer, it is imperative that the TEC of both the new topcoat and the dense reaction layer have as small mismatch as possible with the rest of the TBC system. In addition, the additional or reaction layers are designed as thin as possible. Preferred materials for CMAS barrier layers are, e.g., RE zirconates as $Gd_2Zr_2O_7$, aluminum oxide and high YSZ (Y2O3/ZrO2 solid solutions) (Ref 141-143). It is known that due to the wetting behavior of CMAS slags, infiltration into coarse pore structures occurs at a slower rate compared to fine pores and narrow channels (Ref 144, 145). For this reason, it is advantageous to make the porosity of the layers multimodal: Areas with fine pore structure are capable of rapidly binding CMAS slags. Areas with coarse pore structure with some distance to the surface maintain strain tolerance for a longer period of time. Approaches in this direction have been presented, especially for columnar TBC structures (EB-PVD, PS-PVD, SPS), where CMAS tolerance of systems with different intra-columnar porosity or size of inter-columnar gaps was investigated (Ref 146, 147).

Burner Rig Lifetime of TBC Systems

As mentioned in Introduction, burner rig tests are a relatively cost-effective way to mimic the complex thermo-mechanical loads in a gas turbine environment. Because these tests involve temperature gradients at elevated temperatures with cyclic heating and cooling involving rapid temperature transients, they can be used to study both the temperature-induced aging of the individual layers of the TBC systems at relevant temperatures and the effects of gradient conditions on the effective stress levels resulting from CTE mismatches. By using the hot combustion gases as a heat source and the possibility of adding other media, corrosion phenomena can also be studied to a certain extent in an application-related manner. A disadvantage of the burner rig experiments is to date that these test results are

difficult to cross-reference between different laboratories due to the still incomplete standardization (Ref 148). On the one hand, this is attributable to the fact that the thermomechanical loads on the coatings are more complex on the typically button-shaped specimens (due to the non-negligible influence of the specimen edges) than on cylindrical specimens. On the other hand, various test rig designs are used (Ref 39), which differ noticeably in terms of the heat and force applied to the specimens due to variants of gas burners, cooling concepts and specimen fixtures.

In this paper, we therefore relate the performance of different TBC systems to the lifetime in burner rig experiments from only one/our laboratory to enable a direct comparison. In doing so, we knowingly accept that the best TBC systems in each category worldwide may not be considered. On the other hand, sufficient data are available to allow some general qualitative conclusions. The test conditions were chosen in most cases as follows: substrates were made from IN738 with a button diameter of 30mm and thickness of 3mm. An MCrAlY bond coat of about 150 µm thickness was applied by vacuum plasma spraying (VPS) having a roughness of R_a = 7-8µm. The total thickness of the ceramic topcoats was in the range of about 400-500µm. The surface temperature and the temperature in the substrate center during the heating phases were at about 1400 and 1050 °C, respectively. The dwell times in each cycle were 5min for heating and 2 min for cooling. The setup and experimental procedure of the burner rig test are described in more detail in (Ref 149).

The results are plotted in Fig. 3 as a function of the reciprocal bond coat temperatures. As the major failure mechanism, the TGO growth, is thermally activated, a straight line is often found for each TBC system. First, results of APS coatings having the typical splat-based microstructure are shown by symbols in black color. The comparison of two coating systems produced with modern triplex guns (Triplex II (T2), TriplexPro (TP), Oerlikon Metco, Wohlen, Switzerland), which differ in their microstructure mainly by their porosity (T2 12%–14%, TP 14%–16%), clearly shows the positive influence of higher porosity levels on the lifetime. Taking the current internal standard deposited by TP as reference, the temperature dependence of the lifetimes is plotted as a black line. As mentioned above, this trend is typically found in the case of failures due to delaminations in the TBC/BC interface region, which are essentially driven by the thermally induced growth of the oxide layer (TGO). The lifetime of the segmented system tested was of a similar order to that of the porous APS coatings. This can be interpreted so as that at fairly low layer thickness, the advantage of the higher strain tolerance of the layers will be compensated by the disadvantage of the higher modulus of elasticity of the relatively dense segment structure. For thicker segmented layer, the positive effect of segmentation is certainly more pronounced, so the immediate failure of thick (>1mm) porous coatings was observed in the burner rig test, while segmented thick coatings survived several hundred cycles (Ref 150).

The group of data points in red color includes systems with modified interfaces between the bond coat and ceramic. In the case of TBC systems provided with a flash coat consisting of ODS material (Ref 151), no clear advantage can yet be observed with IN738 as substrate material compared to the single-layer VPS system. In the case of CMSX4 as substrate material, on the other hand, the improvement is clear, partly due to the improved TEC adaptation at the interface (Ref 152). For the APS coatings, which have self-healing particles incorporated in the region close to the bond coat interface, as comparison the dense APS coatings (Triplex II) have to be considered. Compared to these coatings, a rather clear improvement was observed (Ref 153). Of course, in the self-healing TBCs the antagonistic effects of the reacting self-healing particles bridging the growing cracks on the one hand while reducing porosity and strain tolerance at the interface region at the same time have to be well adapted to the specific loading regime to gain a lifetime increase. An improvement of the thermal cyclic performance was also found for a structuring of the bond coat surface, e.g., by laser cladding or laser ablation, detailed results cannot be reported here due to confidentiality, but similar approaches are found in (Ref 154).

Results of TBC systems with columnar microstructure are shown with blue symbols in Fig. 3. It is obvious that single-layer TBCs produced by the SPS process are not competitive in this category at present (Ref 155). This may be attributed to a low fracture toughness in the root region of the columns caused by the growth mechanism during SPS processing in combination with the local out-of-plane stresses at the interface (Ref 156). Much improved strain tolerance and coating adhesion are found in the case of columnar coatings produced by PS-PVD. Here, deposition at comparatively high temperatures on slightly pre-oxidized, polished bond coat layers produces a chemical bonding which, in combination with a higher column density, leads to a significantly longer cyclic life (Ref 157).

The blue shading in Fig. 3 indicates the region where lifetime results of commercial EB-PVD coatings are found, but cannot be published in detail for PI reasons. Similar to the columnar PS-PVD systems, these lifetimes are noticeably higher than the range accessible with typical APS structures. However, it should be noted that the TBC thicknesses in these cases are mostly well below 300µm, which also leads to a lower surface temperature and also lower energy release rates. It is obvious that the lifetime

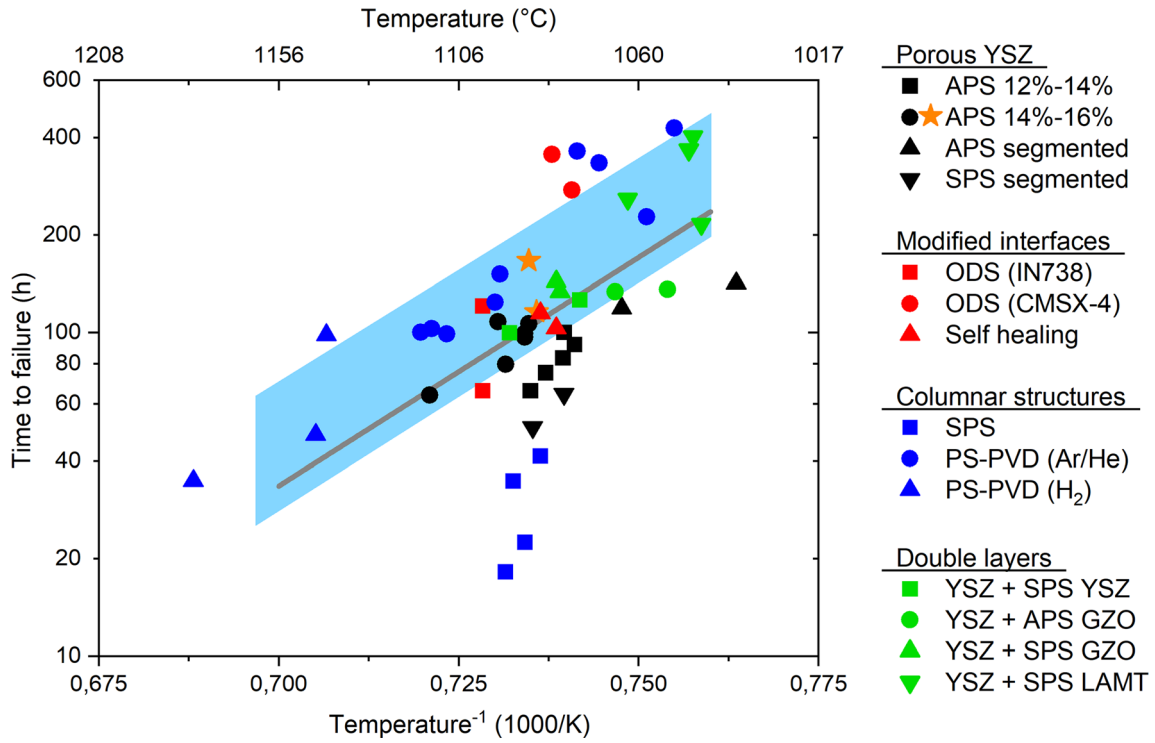

Fig. 3 Results of burner rig tests with 5 min dwell time and surface temperatures of about 1400 °C for different TBC systems as a function of reciprocal bond coat temperature. The star added for APS indicates slower heating/cooling (see text)

data are reached by some thick thermally sprayed TBC systems.

Results from double-layer TBC systems are shown in Fig. 3 with green symbols. It is evident that the cyclic lifetime of double-layer systems with a porous YSZ interlayer made by APS and a columnar top layer deposited by SPS process performs consistently the same or better than a porous single-layer APS TBC. This can be attributed to the fact that here the high fracture toughness of the APS microstructure was successfully combined with reduced driving forces for crack propagation arising from the strain-tolerant columnar SPS top layer and especially the reduction of the local out-of-plane stresses at the APS/SPS interface due to the use of equal materials. Double-layer systems YSZ/GZO with porous APS top layers are inferior to those with columnar SPS top layers of GZO. Here also the extremely good performance of the complex perovskite La(Al1/4Mg1/2Ta1/4)O3 (LAMT) SPS coatings should be mentioned. Although the phase composition changed during cycling, the coating still was intact after up to more than 4800 cycles (Ref 158).

Finally, in Fig. 3 also two data points of APS YSZ topcoats with modified thermal cycles are included (Ref 159). In this case the heating and cooling rates have been reduced (+/- 10K/min). Although the surface temperature was extremely high (~ 1550°C), the lifetime of these coatings were longer than the ones of the other APS TBCs. This clearly indicates the importance of the transient phases of the thermal cycles and is currently the content of further studies.

Short Summary

In the field of processing, especially the deposition techniques with non-line-of-sight capabilities in combination with columnar structures (SPS, PS-PVD) appear to be attractive for the application of TBCs, especially for coatings of complex shaped parts, also, e.g., additively manufactured ones. Improved understanding of the different failure modes compared to APS coatings seems still to be needed. It is worthwhile to note that certain thermal spray coatings (as PS-PVD ones) can show similar lifetimes as EB-PVD coatings under the harsh burner rig tests conditions with extensive TGO growth, however, without additional mechanical load. This is astonishing as the tested thermally sprayed coatings were much thicker than the EB-PVD ones. For high-temperature applications, double-/multilayer approaches with new thermally stable materials combined with tough YSZ used directly on the bond coat will probably be the most reliable approach. These concepts can also mitigate to some extent the CMAS attack using reactive topcoats and appropriate microstructures.

Modifications of the regions close to topcoat/bond coat interface can lead to a considerable improvement of the performance of the system by improving the adhesion (bond coat structuring, adopting of thermal expansion) or reducing crack growth (self-healing concept).

The role of the transient phases during thermal cycling is not fully understood yet, and detailed knowledge might lead to a considerable extension of the operation regime of YSZ.

Outlook

Several thermally sprayed thick coatings (PS-PVD, double-layer SPS) show similar lifetimes as thin EB-PVD coatings. Here it is important to demonstrate that the columnar structure obtained by the thermal spray method can be comparable to EB-PVD microstructures under thermal and mechanical loads as in TGMF testing. Corresponding experiments are planned in the near future.

A huge number of new TBC materials have been suggested and characterized to some extent in the past. It is essential that not only thermophysical properties of new ceramics are evaluated, but also the more application oriented investigations on real coatings are made using harsh, engine like conditions and compare the results to standard, e.g., APS YSZ, coatings.

CMAS will remain a major issue, especially for aero engines for at least the next decade. Certainly, a major part of the present TBC research is focusing on this problem as it is a major source of third party funding. This amount of funding is of course showing that CMAS attack is a major problem for the industry. Some of the advanced TBC materials certainly have potential in mitigating CMAS attack. If these are deposited with adopted porosity distributions, also using new thermal spray methods, further significant progress can be expected.

Although not discussed in too much detail, also due to propriety reasons, the adjustment of the bond coat surface before depositing the topcoat appears to be an excellent way to improve the lifetime and performance of TBCs. Of course, it is known for decades that rough bond coats and also flash coats, which are meanwhile standard for many TBC applications, lead to an improvement. More specific surface structures obtained by, e.g., laser-assisted processes or by optimized spraying processes allow a further significant lifetime increase.

With the increasing need to reduce CO_2 emissions also, hydrogen turbines are attracting more attention. Although the adoption of the combustion process to allow stable operation and to reduce NO_x emissions is a major focus of the research also, materials issues have to be solved including adopted protective coatings (Ref 160). It is obvious that materials issues related to the higher water vapor content, which often increases oxidation rates and volatilization, are important. In addition, more pronounced phase transformation of the YSZ at lower temperatures and a lower cyclic lifetime, especially for heavy cycling, as in aero engines can be observed under wet conditions. Furthermore, also the higher heat transfer to the components has to be considered, which can be addressed by lower conductivity materials in combination with improved temperature capability.

Within the context of increased use of renewables, gas turbines will play an increasing role as load and full-flexible technology to fill the gap between energy demand and production. Here research with respect to TBCs should be focused on the impact of varying operation times and different heating and cooling phases on the lifetime of the coating systems.

Related to this topic, we will certainly further investigate the massive increase in the lifetime of YSZ TBCs by the use of specific transient regimes with medium cooling/heating rates. This might allow the use of YSZ far beyond 1200 °C surface temperature.

Acknowledgment The authors would like to thank all members of the high-temperature department for their strong support of the described developments. In addition, the support with respect to microstructural images from Jana Joeris, Hongbo Guo, Alexandre Guinard, Dapeng Zhou, Denis Koch and Doris Sebold, still or at former times at Forschungszentrum Jülich GmbH, is acknowledged.

Funding Open Access funding enabled and organized by Projekt DEAL.

References

1. C.G. Levi, Emerging Materials and Processes for Thermal Barrier Systems, *Curr. Opin. Solid State Mater. Sci.*, 2004, **8**(1), p 77–91.
2. A. Feuerstein et al., Technical and Economical Aspects of Current Thermal Barrier Coating Systems for Gas Turbine Engines by Thermal Spray and EBPVD: A Review, *J. Therm. Spray Technol.*, 2008, **17**(2), p 199–213.

3. C.U. Hardwicke and Y.-C. Lau, Advances in Thermal Spray Coatings for Gas Turbines and Energy Generation: A Review, *J. Therm. Spray Technol.*, 2013, **22**(5), p 564–576.
4. R.A. Miller, Current Status of Thermal Barrier Coatings- An Overview, *Surf. Coat. Tech.*, 1987, **30**(1), p 1–11.
5. R. Vaßen et al., Overview on Advanced Thermal Barrier Coatings, *Surf. Coat. Technol.*, 2010, **205**(4), p 938–942.
6. E. Bakan and R. Vaßen, Ceramic Top Coats of Plasma-Sprayed Thermal Barrier Coatings: Materials, Processes, and Properties, *J. Therm. Spray Technol.*, 2017, **26**(6), p 992–1010.
7. Wahl, J.B. and K. Harris. Superalloys in Industrial Gas Turbines - An Overview. In: *Presented at the 9th World Conference on Investment Casting, October 13-16, 1996, San Francisco, CA USA*
8. D.R. Clarke and C.G. Levi, Materials Design For The Next Generation Thermal Barrier Coatings, *Annu. Rev. Mater. Res.*, 2003, **33**(1), p 383–417.
9. V. Arnault et al., Thermal Barrier Coatings for Aircraft Turbine Airfoils: Thermal Challenge and Materials, *Revue de Metallurgie. Cahiers D'Informations Techniques*, 1999, **96**(5), p 585–597.
10. Meier, S.M., D.M.N., Sheffler, K.D. *Thermal barrier coating life prediction model development, Phase II Final Report*, in *Contract NAS3-23944, NASA CR 189111*. (1991)
11. R. Vaßen, G. Kerkhoff and D. Stöver, Development of a Micromechanical Life Prediction Model for Plasma Sprayed Thermal Barrier Coatings, *Materials science and engineering / A*, 2001, **303**, p 100–109.
12. X. Zhang et al., Constrained Sintering and Cracking of Air Plasma Sprayed Thermal Barrier Coatings: Experimental Observation and Modeling, *J. Am. Ceram. Soc.*, 2021, **104**(9), p 4759–4772.
13. D. Naumenko et al., Failure Mechanisms of Thermal Barrier Coatings on MCrAlY-type Bondcoats Associated with the Formation of the Thermally Grown Oxide, *J. Mater. Sci.*, 2009, **44**(7), p 1687–1703.
14. C. Nordhorn et al., Probabilistic Lifetime Model for Atmospherically Plasma Sprayed Thermal Barrier Coating Systems, *Mech. Mater.*, 2016, **93**, p 199–208.
15. Warren, P., et al. *Modeling Thermally Grown Oxides in Thermal Barrier Coatings Using Koch Fractals* in *ASME Turbo Expo: Turbomachinery Technical Conference and Exposition*. 2019. Phoenix, AZ
16. M. Baker and P. Seiler, A Guide to Finite Element Simulations of Thermal Barrier Coatings, *J. Therm. Spray Technol.*, 2017, **26**(6), p 1146–1160.
17. Bose, S., *High Temperature Coatings*. (2011): Elsevier Science
18. Stecura, S., *Effects of Compositional Changes on the Performance of a Thermal Barrier Coating System*. 1978, NASA TM-78976, National Aeronautics and Space Administration
19. R.A. Miller, Thermal Barrier Coatings for Aircraft Engines: History and Directions, *J. Therm. Spray Technol.*, 1997, **6**(1), p 35–42.
20. S. Bose and J. DeMasiMarcin, Thermal Barrier Coating Experience in Gas Turbine Engines at Pratt & Whitney, *J. Therm. Spray Technol.*, 1997, **6**(1), p 99–104.
21. U. Schulz et al., Review on Advanced EB-PVD Ceramic Topcoats for TBC Applications, *Int. J. Appl. Ceram. Tec.*, 2004, **1**(4), p 302–315.
22. R. Darolia, Thermal Barrier Coatings Technology: Critical Review, Progress Update, Remaining Challenges and Prospects, *Int. Mater. Rev.*, 2013, **58**(6), p 315–348.
23. Chevalier, J., et al., Forty Years after the Promise of «ceramic steel?»: Zirconia-based Composites with a Metal-like Mechanical Behavior. J. Am. Ceramic Soc. (2019)
24. C. Mercer et al., On a Ferroelastic Mechanism Governing the Toughness of Metastable Tetragonal-Prime Yttria-Stabilized Zirconia, *Proceedings of the Royal Society of London A: Mathematical, Physical and Engineering Sciences*, 2007, **463**(2081), p 1393–1408.
25. D.M. Lipkin et al., Phase Evolution Upon Aging of Air-plasma sprayed t′-zirconia Coatings: I - Synchrotron x-ray Diffraction, *J. Am. Ceram. Soc.*, 2013, **96**(1), p 290–298.
26. A. Sharma et al., Interplay of the Phase and the Chemical Composition of the Powder Feedstock on the Properties of Porous 8YSZ Thermal Barrier Coatings, *J. Eur. Ceram. Soc.*, 2021, **41**(6), p 3706–3716.
27. R. Vaßen, F. Träger and D. Stöver, New Thermal Barrier Coatings Based on Pyrochlore/YSZ Double-Layer Systems, *Int. J. Appl. Ceram. Tec.*, 2004, **1**(4), p 351–361.
28. H. Dai et al., Thermal Stability of Double-Ceramic-Layer Thermal Barrier Coatings with Various Coating Thickness, *Mater. Sci. Eng., A*, 2006, **433**(1), p 1–7.
29. Z.Y. Shen et al., LZC/YSZ DCL TBCs by EB-PVD: Microstructure, Low Thermal Conductivity and High Thermal Cycling Life, *J. Eur. Ceram. Soc.*, 2019, **39**(4), p 1443–1450.
30. Kadam, N.R., G. Karthikeyan, and D.M. Kulkarni. Effect of Spray Angle onto the Microstructure of EB-PVD enabled 8YSZ Thermal Barrier Coatings. In: *11th International Conference on Materials, Processing and Characterization (ICMPC)*. (2020). Indore, INDIA
31. M. Peters et al., EB-PVD Thermal Barrier Coatings for Aeroengines and Gas Turbines, *Adv. Eng. Mater.*, 2001, **3**(4), p 193–204.
32. P.G. Lashmi et al., Present Status and Future Prospects of Plasma Sprayed Multilayered Thermal Barrier Coating Systems, *J. Eur. Ceram. Soc.*, 2020, **40**(8), p 2731–2745.
33. J.T. Demasimarcin and D.K. Gupta, PROTECTIVE COATINGS IN THE GAS-TURBINE ENGINE, *Surf. Coat. Technol.*, 1994, **68**, p 1–9.
34. *Final Report Summary - TOPPCOAT (Towards design and processing of advanced, competitive thermal barrier coating systems)*. https://cordis.europa.eu/project/id/516149/reporting/de.
35. Poerschke, D.L., Jackson, R.W., Levi, C.G. Silicate Deposit Degradation of Engineered Coatings in Gas Turbines: Progress Toward Models and Materials Solutions, In: *Annual Review of Materials Research, Vol 47*, D.R. Clarke, Editor. 2017. p. 297-330
36. D. Naumenko et al., Overview on Recent Developments of Bondcoats for Plasma-Sprayed Thermal Barrier Coatings, *J. Therm. Spray Technol.*, 2017, **26**(8), p 1743–1757.
37. H. Nickel et al., Development of NiCrAlY Alloys for Corrosion-resistant Coatings and Thermal Barrier Coatings of Gas Turbine Components, *J Pressure Vessel Technol-Trans Asme*, 1999, **121**(4), p 384–387.
38. R. Eriksson et al., TBC Bond coat-top Coat Interface Roughness: INFLUENCE on Fatigue Life and Modelling Aspects, *Surf. Coat. Technol.*, 2013, **236**, p 230–238.
39. R. Vaßen et al., Overview in the Field of Thermal Barrier Coatings Including Burner Rig Testing in the European Union, *Seramikkusu*, 2008, **43**, p 371–381.
40. K.Y. Park et al., Variation of Thermal Barrier Coating Lifetime Characteristics with Thermal Durability Evaluation Methods, *J. Therm. Spray Technol.*, 2018, **27**(8), p 1436–1446.
41. Bartsch, M., et al., *THE ROLE OF CYCLIC MECHANICAL LOADING AND THERMAL GRADIENTS IN DAMAGE BEHAVIOR OF THERMAL BARRIER COATING SYSTEMS*, in *Advances in Ceramic Coatings and Ceramic-Metal Systems*, D. Zhu and K. Plucknett, Editors. (2005). p. 103-110

42. F. Traeger et al., Thermal Cycling Setup for Testing Thermal Barrier Coatings, *Adv. Eng. Mater.*, 2003, **5**(6), p 429–432.
43. T.A. Schaedler et al., Toughening of Nontransformable t′-YSZ by Addition of Titania, *J. Am. Ceram. Soc.*, 2007, **90**(12), p 3896–3901.
44. J.A. Krogstad, M. Lepple and C.G. Levi, Opportunities for Improved TBC Durability in the CeO2–TiO2–ZrO2 System, *Surf. Coat. Technol.*, 2013, **221**, p 44–52.
45. J. Wang et al., Phase Stability and Thermo-physical Properties of ZrO2-CeO2-TiO2 Ceramics for Thermal Barrier Coatings, *J. Eur. Ceram. Soc.*, 2018, **38**(7), p 2841–2850.
46. S. Raghavan et al., Ta2O5/Nb2O5 and Y2O3 Co-doped Zirconias for Thermal Barrier Coatings, *J. Am. Ceram. Soc.*, 2004, **87**(3), p 431–437.
47. J. Wang et al., Influence of Gd2O3 Substitution on Thermal and Mechanical Properties of ZrO2-Ta2O5-Y2O3, *J. Eur. Ceram. Soc.*, 2021, **41**(2), p 1654–1663.
48. R. Taylor, J.R. Brandon and P. Morrell, Microstructure, Composition and Property Relationships of Plasma-Sprayed Thermal Barrier Coatings, *Surf. Coat. Technol.*, 1992, **50**(2), p 141–149.
49. D. Zhu and R.A. Miller, Development of Advanced Low Conductivity Thermal Barrier Coatings, *Int. J. Appl. Ceram. Technol.*, 2004, **1**(1), p 86–94.
50. D. Zhu et al., Furnace Cyclic Oxidation Behavior of Multicomponent Low Conductivity Thermal Barrier Coatings, *J. Therm. Spray Technol.*, 2004, **13**(1), p 84–92.
51. D. Chen et al., Microstructure, Thermal Characteristics, and Thermal Cycling Behavior of the Ternary Rare earth Oxides (La2O3, Gd2O3, and Yb2O3) co-doped YSZ Coatings, *Surface and Coatings Technol*, 2020, **403**, p 126387.
52. R. Vaßen et al., Zirconates as New Materials for Thermal Barrier Coatings, *J. Am. Ceram. Soc.*, 2000, **83**(8), p 2023–2028.
53. H. Lehmann et al., Thermal Conductivity and Thermal Expansion Coefficients of the Lanthanum Rare-Earth-Element Zirconate System, *J. Am. Ceram. Soc.*, 2003, **86**(8), p 1338–1344.
54. G. Suresh et al., Investigation of the Thermal Conductivity of Selected Compounds of Lanthanum, *Samarium and Europium. J. Alloys Compd.*, 1998, **269**(1–2), p L9–L12.
55. Z. Qu, C. Wan and W. Pan, Thermal Expansion and Defect Chemistry of MgO-Doped Sm2Zr2O7, *Chem. Mater.*, 2007, **19**(20), p 4913–4918.
56. G. Suresh et al., Investigation of the Thermal Conductivity of Selected Compounds of Gadolinium and Lanthanum, *J. Nucl. Mater.*, 1997, **249**(2), p 259–261.
57. Jing Dong Wang, W.P., Qiang Xu Kazutaka Mori Taiji Torigoe, *Thermal Conductivity of the New Candidate Materials for Thermal Barrier Coatings.* Key Engineering Materials, (2007). **280-283**: p. 1503-1506
58. Y.X. Qin et al., Low Thermal Conductivity Ceramics for Thermal Barrier Coatings, *Key Eng. Mater.*, 2007, **336–338**, p 1764–1766.
59. X. Cao et al., Lanthanum-Cerium Oxide as a Thermal Barrier-Coating Material for High-Temperature Applications, *Adv. Mater.*, 2003, **15**(17), p 1438–1442.
60. Z. Qu, C. Wan and W. Pan, Thermophysical Properties of Rare-earth Stannates: Effect of Pyrochlore Structure, *Acta Mater.*, 2012, **60**(6–7), p 2939–2949.
61. L. Chen et al., Thermo-Mechanical Properties of Fluorite Yb3TaO7 and Yb3NbO7 Ceramics with Glass-like Thermal Conductivity, *J. Alloy. Compd.*, 2019, **788**, p 1231–1239.
62. F. Cernuschi et al., Thermo-Physical Properties of as Deposited and Aged Thermal Barrier Coatings (TBC) for Gas Turbines: State-of-the Art and Advanced TBCs, *J. Eur. Ceram. Soc.*, 2018, **38**(11), p 3945–3961.
63. J. Yang et al., A Promising Material for Thermal Barrier Coating: Pyrochlore-Related Compound Sm2FeTaO7, *Scripta Mater.*, 2018, **149**, p 49–52.
64. Z. Xue, Y. Ma and H. Guo, Synthesis, Thermal Conductivities and Phase Stability of Gd3TaO7 and La doped Gd3TaO7 Ceramics, *J. Alloy. Compd.*, 2018, **732**, p 759–764.
65. G. Lan et al., A Complete Computational Route to Predict Reduction of Thermal Conductivities of Complex Oxide Ceramics by Doping: A Case Study of La2Zr2O7, *J. Alloys and Compound.*, 2020, **826**, p 154224.
66. W. Ma et al., Perovskite-Type Strontium Zirconate as a New Material for Thermal Barrier Coatings, *J. Am. Ceram. Soc.*, 2008, **91**(8), p 2630–2635.
67. Y. Liu et al., Theoretical and Experimental Investigations on High Temperature Mechanical and Thermal Properties of BaZrO3, *Ceram. Int.*, 2018, **44**(14), p 16475–16482.
68. M.O. Jarligo et al., Application of Plasma-Sprayed Complex Perovskites as Thermal Barrier Coatings, *J. Therm. Spray Technol.*, 2009, **18**(2), p 187–193.
69. H. Guo et al., Thermo-Physical and Thermal Cycling Properties of Plasma-Sprayed $BaLa_2Ti_3O_{10}$ Coating as Potential Thermal Barrier Materials, *Surf. Coat. Technol.*, 2009, **204**(5), p 691–696.
70. J. Yuan et al., SrCeO3 as a Novel Thermal Barrier Coating Candidate for High–Temperature Applications, *J. Alloy. Compd.*, 2018, **740**, p 519–528.
71. E. Li et al., The Effect of Al3+ Doping on the Infrared Radiation and Thermophysical Properties of SrZrO3 Perovskites as Potential Low Thermal Infrared Material, *Acta Materialia*, 2021, **209**, p 116795.
72. Bansal, N.P., D. Zhu, and M. Eslamloo-Grami, *Thermal Properties of Oxides With Magnetolumbite Structure for Advanced Thermal Barrier Coatings* in *NASA Technical Memorandum*. 2007: Sixth International Conference on High Temperature Ceramic Matrix Composites (HTCMC-6).
73. G. Pracht, R. Vaßen and D. Stöver, Lanthanum-Lithium Hexaaluminate—A New Material for Thermal Barrier Coatings in Magnetoplumbite Structure—Material and Process Development, *Ceram. Eng. Sci. Proc.*, 2009, **27**, p 87–99.
74. A. Morán-Ruiz et al., Comparison of the Thermal Resistance Behaviour of Synthesized Ln4Al2O9 (Ln = Y, Sm, Eu, Gd, Tb) Materials vs Commercial Zr0.8Y0.2O1.9 (8YSZ), *Surface and Coatings Technol.*, 2019, **374**, p 745–751.
75. A. Du et al., Thermal Conductivity of Monazite-Type REPO4 (RE=La, Ce, Nd, Sm, Eu, Gd), *J. Am. Ceram. Soc.*, 2009, **92**(11), p 2687–2692.
76. L. Guo et al., GdPO4 as a Novel Candidate for Thermal Barrier Coating Applications at Elevated Temperatures, *Surf. Coat. Technol.*, 2018, **349**, p 400–406.
77. K.W. Schlichting, N.P. Padture and P.G. Klemens, Thermal Conductivity of Dense and Porous Yttria-Stabilized Zirconia, *J. Mater. Sci.*, 2001, **36**(12), p 3003–3010.
78. H. Hayashi et al., Thermal Expansion Coefficient of Yttria Stabilized Zirconia for Various Yttria Contents, *Solid State Ionics*, 2005, **176**(5–6), p 613–619.
79. J.R. Nicholls et al., Methods to Reduce the Thermal Conductivity of EB-PVD TBCs, *Surf. Coat. Technol.*, 2002, **151–152**, p 383–391.
80. E. Bakan et al., Gadolinium Zirconate/YSZ Thermal Barrier Coatings: Plasma Spraying, Microstructure, and Thermal Cycling Behavior, *J. Am. Ceram. Soc.*, 2014, **97**(12), p 4045–4051.
81. M. Frommherz et al., Gadolinium zirconate/YSZ thermal Barrier Coatings: Mixed-Mode Interfacial Fracture Toughness and Sintering Behavior, *Surf. Coat. Technol.*, 2016, **286**, p 119–128.

82. S. Mahade et al., Failure Analysis of Gd2Zr2O7/YSZ Multi-Layered Thermal Barrier Coatings Subjected to Thermal Cyclic Fatigue, *J. Alloy. Compd.*, 2016, **689**, p 1011–1019.
83. B. Cheng et al., Gradient Thermal Cyclic Behaviour of La2Zr2O7/YSZ DCL-TBCs with Equivalent Thermal Insulation Performance, *J. Eur. Ceram. Soc.*, 2018, **38**(4), p 1888–1896.
84. A. Kulkarni et al., Processing Effects on Porosity-Property Correlations in Plasma Sprayed Yttria-Stabilized Zirconia Coatings, *Mater. Sci. Eng., A*, 2003, **359**(1), p 100–111.
85. G. Witz et al., Phase Evolution in Yttria-Stabilized Zirconia Thermal Barrier Coatings Studied by Rietveld Refinement of x-ray Powder Diffraction Patterns, *J. Am. Ceram. Soc.*, 2007, **90**(9), p 2935–2940.
86. E. Bakan et al., Porosity-Property Relationships of Plasma-Sprayed Gd2Zr2O7/YSZ Thermal Barrier Coatings, *J. Am. Ceram. Soc.*, 2015, **98**(8), p 2647–2654.
87. O. Aranke et al., Microstructural Evolution and Sintering of Suspension Plasma-Sprayed Columnar Thermal Barrier Coatings, *J. Therm. Spray Technol.*, 2019, **28**(1), p 198–211.
88. J. Yan et al., Sintering Modeling of Thermal Barrier Coatings at Elevated Temperatures: A Review of Recent Advances, *Coatings*, 2021, **11**(10), p 1214.
89. C.M. Rost et al., Entropy-Stabilized Oxides, *Nature Communications*, 2015, **6**, p 8485.
90. J. Liu et al., Design and synthesis of chemically complex ceramics from the perspective of entropy, *Mater Today Adv*, 2020, **8**, p 100114.
91. G. Anand et al., Phase Stability and Distortion in High-entropy Oxides, *Acta Mater.*, 2018, **146**, p 119–125.
92. R. Djenadic et al., Multicomponent Equiatomic Rare Earth Oxides, *Materials Research Letters*, 2017, **5**(2), p 102–109.
93. K. Chen et al., A Five-Component Entropy-Stabilized Fluorite Oxide, *J. Eur. Ceram. Soc.*, 2018, **38**(11), p 4161–4164.
94. J. Gild et al., High-Entropy Fluorite Oxides, *J. Eur. Ceram. Soc.*, 2018, **38**(10), p 3578–3584.
95. M. Pianassola et al., Solid-State Synthesis of Multicomponent Equiatomic Rare-Earth Oxides, *J. Am. Ceram. Soc.*, 2020, **103**(4), p 2908–2918.
96. A.J. Wright et al., From High-Entropy Ceramics to Compositionally-Complex Ceramics: A Case Study of Fluorite Oxides, *J. Eur. Ceram. Soc.*, 2020, **40**(5), p 2120–2129.
97. L. Xu et al., A New Class of High-Entropy Fluorite Oxides with Tunable Expansion Coefficients, Low Thermal Conductivity and Exceptional Sintering Resistance, *J. Eur. Ceram. Soc.*, 2021, **41**(13), p 6670–6676.
98. L. Xu et al., Tuning Stoichiometry of High-Entropy Oxides for tailorable thermal expansion coefficients and low thermal conductivity, *J. Am. Ceram. Soc.*, 2021 https://doi.org/10.1111/jace.18155
99. Z. Teng et al., Synthesis and Structures of High-entropy Pyrochlore Oxides, *J. Eur. Ceram. Soc.*, 2020, **40**(4), p 1639–1643.
100. Z. Zhao et al., (La0.2Ce0.2Nd0.2Sm0.2Eu0.2)2Zr2O7: A Novel High-entropy Ceramic with Low Thermal Conductivity and Sluggish Grain Growth Rate, *J Materials Sci Technol*, 2019, **35**, p 2647–2651.
101. J. Dąbrowa et al., Synthesis and Microstructure of the (Co, Cr, Fe, Mn, Ni)3O4 High Entropy Oxide Characterized by Spinel Structure, *Mater. Lett.*, 2018, **216**, p 32–36.
102. Z. Grzesik et al., Defect Structure and Transport Properties of (Co, Cr, Fe, Mn, Ni)3O4 Spinel-Structured High Entropy Oxide, *J. Eur. Ceram. Soc.*, 2020, **40**(3), p 835–839.
103. S. Jiang et al., A New Class of High-Entropy Perovskite Oxides, *Scripta Mater.*, 2018, **142**, p 116–120.
104. A. Sarkar et al., Rare Earth and Transition Metal based Entropy Stabilised Perovskite Type Oxides, *J. Eur. Ceram. Soc.*, 2018, **38**(5), p 2318–2327.
105. Z. Zhao et al., High-Entropy (Y0.2Nd0.2Sm0.2Eu0.2Er0.2)-AlO3: A Promising Thermal/Environmental Barrier Material for Oxide/Oxide Composites, *J. Mater. Sci. Technol.*, 2020, **47**, p 45–51.
106. M. Lim et al., Influence of Mass and Charge Disorder on the Phonon Thermal Conductivity of Entropy Stabilized Oxides Determined by Molecular Dynamics Simulations, *Journal of Applied Physics*, 2019, **125**(5), p 055105.
107. S.V. Divinski et al., A Mystery of "Sluggish Diffusion" in High-Entropy Alloys: The Truth or a Myth?, *Diffusion Foundations*, 2018, **17**, p 69–104.
108. K. Ren et al., Multicomponent High-entropy Zirconates with Comprehensive Properties for Advanced Thermal Barrier Coating, *Scripta Mater.*, 2020, **178**, p 382–386.
109. D. Song et al., Glass-like Thermal Conductivity in Mass-disordered High-entropy (Y, Yb)2(Ti, Zr, Hf)2O7 for Thermal Barrier Material, *Materials & Design*, 2021, **210**, p 110059.
110. Fauchais, P.L., J.V.R. Heberlein, and M. Boulos, *Thermal Spray Fundamentals: From Powder to Part*. 2014: Springer.
111. R. Vaßen et al., Performance of YSZ and $Gd_2Zr_2O_7$/YSZ Double Layer Thermal Barrier coatings in Burner Rig Tests, *J. Eur. Ceram. Soc.*, 2020, **40**, p 480–490.
112. Vaßen, R., E. Bakan, and S. Schwartz-Lückge, *Influence of Substrate Removal Method on the Properties of Free-Standing YSZ Coatings.* Coatings, 2021. **11**(499).
113. W. Chi, S. Sampath and H. Wang, Ambient and High-temperature Thermal Conductivity of Thermal Sprayed Coatings, *J. Therm. Spray Technol.*, 2006, **15**(4), p 773–778.
114. Akoshima, M. and S. Takahashi, *Anisotropic Thermal Diffusivities of Plasma-Sprayed Thermal Barrier Coatings.* International Journal of Thermophysics, (2017). **38**(9).
115. Ghasripoor F., S.R., Dorfman M., *Abradables Improve Gas Turbine Efficiency.* Materials World, 1997: p. 328-330.
116. Cui, Y.J., et al., *Evolution of the Residual Stress in Porous Ceramic Abradable Coatings Under Thermal Exposure.* Surface & Coatings Technology, 2020. **394**.
117. A. Scrivani et al., Thermal Fatigue Behavior of Thick and Porous Thermal Barrier Coatings Systems, *J. Therm. Spray Technol.*, 2007, **16**(5–6), p 816–821.
118. M. Arai and T. Suidzu, Porous Ceramic Coating for Transpiration Cooling of Gas Turbine Blade, *J. Therm. Spray Technol.*, 2013, **22**(5), p 690–698.
119. Fournier, V., et al., *Plasma Spraying of Mullite and Pore Formers for Thermal Insulating Applications.* Surface & Coatings Technology, (2021). **406**.
120. Wigren, J. and L. Pejryd, *Thermal barrier coatings - Why, how, where and where to*. THERMAL SPRAY, VOLS 1 AND 2: MEETING THE CHALLENGES OF THE 21ST CENTURY. (1998) p. 1531-1542.
121. H.B. Guo, R. Vaßen and D. Stöver, Atmospheric Plasma Sprayed Thick Thermal Barrier Coatings with High Segmentation Crack Density, *Surf. Coat. Technol.*, 2004, **186**(3), p 353–363.
122. S.V. Shinde et al., Segmentation Crack Formation Dynamics during Air Plasma Spraying of Zirconia, *Acta Mater.*, 2020, **183**, p 196–206.
123. P. Bengtsson, T. Ericsson and J. Wigren, Thermal Shock Testing of Burner Cans Coated with a Thick Thermal Barrier Coating, *J. Therm. Spray Technol.*, 1998, **7**(3), p 340–348.
124. D. Schwingel et al., Mechanical and Thermophysical Properties of Thick PYSZ Thermal Barrier Coatings: Correlation with Microstructure and Spraying Parameters, *Surf. Coat. Technol.*, 1998, **108**(1–3), p 99–106.
125. Czech, N., *Einsatz von Wärmedämmschichten in stationären Gasturbinen.* cfi/Ber. DKG, (2000). **77**(9): p. 18-21.

126. Subramanian, R., A. Burns, and W. Stamm. *Advanced Multifunctional Coatings for Land-based Industrial Gas Turbines*. In: *ASME Turbo Expo 2008: Power for Land, sea and Air*. 2008. June 9-13, 2008, Berlin, Germany: ASME, New York.
127. K. Mondal et al., Thermal Barrier Coatings Overview: Design, Manufacturing, and Applications in High-Temperature Industries, *Ind. Eng. Chem. Res.*, 2021, **60**(17), p 6061–6077.
128. Q.M. Liu, S.Z. Huang and A.J. He, Composite Ceramics Thermal Barrier Coatings of Yttria Stabilized Zirconia for Aero-Engines, *J. Mater. Sci. Technol.*, 2019, **35**(12), p 2814–2823.
129. M. Aghasibeig et al., A Review on Suspension Thermal Spray Patented Technology Evolution, *J. Therm. Spray Technol.*, 2019, **28**(7), p 1579–1605.
130. Vaßen, R., et al., *Suspension Plasma Spraying: Process Development and Applications*, In: *Thermal Spray 2009: Proceedings of the International Thermal Spray Conference / ed.: B.R. Marple, M.M. Hyland, Y.-C. Lau, C.-J. Li, R.S. Lima, G. Montavon. - S. 162 - 167*. (2009).
131. K. VanEvery et al., Column Formation in Suspension Plasma-Sprayed Coatings and Resultant Thermal Properties, *J. Therm. Spray Technol.*, 2011, **20**(4), p 817–828.
132. N. Curry et al., Thermal Conductivity Analysis and Lifetime Testing of Suspension Plasma-Sprayed Thermal Barrier Coatings, *Coatings*, 2014, **4**(3), p 630.
133. B. Bernard et al., Effect of Suspension Plasma-Sprayed YSZ Columnar Microstructure and Bond Coat Surface Preparation on Thermal Barrier Coating Properties, *J Therm Spray Tech*, 2017, **26**, p 1025–1037.
134. N. Kumar et al., Columnar Thermal Barrier Coatings Produced by Different Thermal Spray Processes, *J. Therm. Spray Technol.*, 2021, **30**(6), p 1437–1452.
135. K..v Niessen, M. Gindrat and A. Refke, Vapor Phase Deposition Using Plasma Spray-PVD, *J. Therm. Spray Technol.*, 2010, **19**(1–2), p 502–509.
136. W. He et al., Advanced Crystallographic Study of the Columnar Growth of YZS Coatings Produced by PS-PVD, *J. Eur. Ceram. Soc.*, 2018, **38**(5), p 2449–2453.
137. D. Marcano et al., Plasma Spray-Physical Vapor Deposition of La1-xSrxCoyFe1-yO3-δ OxygenTransport Membranes on Porous Metallic Supports: Controlling Stress State andPhase Composition, *International Thermal Spray Conference*. ASM International, Long Beach, CA, USA, 2015, p 1121–1127
138. Bakan, E., G. Mauer, and R. Vassen. An assessment of thermal spray technologies for deposition for environmental barrier coatings (EBC). in Thermal Spray paves the Way to the Stars! International Thermal Spray Conference and Exhibition, *Düsseldorf*, DVS Media GmbH, Germany, 2017.
139. C.G. Levi et al., Environmental Degradation of Thermal-Barrier Coatings by Molten Deposits, *MRS Bull.*, 2012, **37**(10), p 932–941.
140. D.L. Poerschke, R.W. Jackson and C.G. Levi, Silicate Deposit Degradation of Engineered Coatings in Gas Turbines: Progress Toward Models and Materials Solutions, *Annu. Rev. Mater. Res.*, 2017, **47**(1), p 297–330.
141. A. Aygun et al., Novel thermal barrier coatings that are resistant to high-temperature attack by glassy deposits, *Acta Mater.*, 2007, **55**(20), p 6734–6745.
142. Mohan, P., et al., *Degradation of Thermal Barrier Coatings by Fuel Impurities and CMAS: Thermochemical Interactions and Mitigation Approaches.* Journal of Thermal Spray Technology, 2009.
143. N.K. Eils, P. Mechnich and W. Braue, Effect of CMAS Deposits on MOCVD Coatings in the System Y2O3–ZrO2: Phase Relationships, *J. Am. Ceram. Soc.*, 2013, **96**(10), p 3333–3340.
144. X. Shan et al., Pore Filling Behavior of YSZ under CMAS Attack: Implications for Designing Corrosion-Resistant Thermal Barrier Coatings, *J. Am. Ceram. Soc.*, 2018, **101**(12), p 5756–5770.
145. D.E. Mack et al., Evolution of Porosity, Crack Density, and CMAS Penetration in Thermal Barrier Coatings Subjected to Burner rig Testing, *J. Am. Ceram. Soc.*, 2019, **102**(10), p 6163–6175.
146. R. Naraparaju et al., Tailoring the EB-PVD Columnar Microstructure to Mitigate the Infiltration of CMAS in 7YSZ Thermal Barrier Coatings, *J. Eur. Ceram. Soc.*, 2017, **37**(1), p 261–270.
147. S. Rezanka et al., Investigation of the Resistance of Open-column-structured PS-PVD TBCs to Erosive and High-Temperature Corrosive Attack, *Surf. Coat. Technol.*, 2017, **324**, p 222–235.
148. ISO, *Test Method of Cyclic Heating for Thermal-Barrier Coatings under Temperature gradient*, In: *Metallic and Other Inorganic Coatings*, ISO, Editor. 2011, ISO. p. 14.
149. F. Traeger et al., Thermal Cycling Setup for Testing Thermal Barrier Coatings, *Adv. Eng. Mater.*, 2003, **5**, p 429–432.
150. M. Karger, R. Vaßen and D. Stöver, Atmospheric Plasma Sprayed Thermal Barrier Coatings with High Segmentation Crack Densities: Spraying Process, Microstructure and Thermal Cycling Behavior, *Surf. Coat. Technol.*, 2011, **206**(1), p 16–23.
151. J. Bergholz et al., Fabrication of Oxide Dispersion Strengthened Bond Coats with Low Al2O3 Content, *J. Therm. Spray Technol.*, 2017, **26**(5), p 868–879.
152. C. Vorkötter et al., Superior Cyclic Life of Thermal Barrier Coatings with Advanced Bond Coats on Single-Crystal Superalloys, *Surf. Coat. Technol.*, 2019, **361**, p 150–158.
153. Koch, D., D.E. Mack, and R. Vaßen, *Degradation and Lifetime of Self-healing Thermal Barrier Coatings in Thermo-Cycling Testing.* to be published.
154. R. Kromer et al., Laser Surface Texturing to Enhance Adhesion Bond Strength of Spray Coatings – Cold Spraying, Wire-arc Spraying, and Atmospheric Plasma Spraying, *Surf. Coat. Technol.*, 2018, **352**, p 642–653.
155. Kumar, N., et al., *Columnar Thermal Barrier Coatings Produced by Different Thermal Spray Processes.* Journal of Thermal Spray Technology, 2021.
156. Zhou, D., et al., *Architecture Designs for Extending Thermal Cycling Lifetime of Suspension Plasma Sprayed Thermal Barrier Coatings.* Ceramics International, 2019.
157. S. Rezanka, G. Mauer and R. Vaßen, Improved Thermal Cycling Durability of Thermal Barrier Coatings Manufactured by PS-PVD, *J. Therm. Spray Technol.*, 2014, **23**(1), p 182–189.
158. N. Schlegel et al., Cycling Performance of a Columnar-Structured Complex Perovskite in a Temperature Gradient Test, *J. Therm. Spray Technol.*, 2015, **24**(7), p 1205–1212.
159. R. Vassen et al., Unique Performance of Thermal Barrier Coatings Made of Yttria-Stabilized Zirconia at Extreme Temperatures (>1500 Degrees C), *J. Am. Ceram. Soc.*, 2021, **104**(1), p 463–471.
160. Stefan, E., et al., *Materials Challenges in Hydrogen-fuelled Gas Turbines.* International Mater. Rev. 2021: p. 1-26.